Project No. 037005

CECILIA

Central and Eastern Europe Climate Change Impact and Vulnerability Assessment

Specific targeted research project

1.1.6.3.I.3.2: Climate change impacts in central-eastern Europe

D4.5
Sensitivity experiments investigating specific feedback processes (in particular land-atmosphere coupling) and their analysis (ICTP, ETH, CUNI, NMA)

Due date of deliverable: 1st October 2009
Actual submission date: 31st December 2009

Start date of project: 1st June 2006 Duration: 43 months

Lead contractor for this deliverable: ICTP

Project co-funded by the European Commission within the Sixth Framework Programme (2002-2006)		
Dissemination Level		
PU	Public	X
PP	Restricted to other programme participants (including the Commission Services)	
RE	Restricted to a group specified by the consortium (including the Commission Services)	
CO	Confidential, only for members of the consortium (including the Commission Services)	

1. The role of land-atmosphere interaction in the increase of climate temperature variability over Europe

The purpose of these sensitivity experiments was to isolate specifically the role of land–atmosphere coupling in projected changes in interannual climate variability during the extratropical summer season following the work of Seneviratne et al. (2006) and Koster et al. (2004). Changes in climate variability is a very important factor for life and society more than it is the change of mean climate since climate variability is related to extreme climate events that are those who most influence human life.

1.1 Data and methodology

For this purpose ICTP conducted two different RCM simulations one with coupled land-atmosphere and one uncoupled in which the soil moisture has been kept to its monthly climatological value.
The coupled simulation is the original 25 km transient simulation delivered from ICTP for the CECILIA project in WP1 deliverable D1.4. This simulation uses as lateral boundary conditions fields from one of the CMIP3 model simulations performed with the global model ECHAM5. The simulated period was 1950-2100 with the SRES-A1B radiative forcing from 2000 onwards.
The uncoupled simulation has been completed with the same model but in a time slice mode. Only the summer months of June, July, August (JJA) have been simulated for the three 30 years time slice 1961-90, 2021-2051 and 2071-2100. In this simulation the soil moisture value has been fixed to the monthly climatological values derived from the 30 years average of the coupled simulation.

The same kind of simulations with the same RCM model have been conducted by NMA at 10 km resolution for the Romanian domain. For this domain and for this resolution only the present day and far future time slice has been considered and the only for the period 1981-88 and 2093-2099.

1.2 Impact of land-atmosphere coupling on summer temperature variability change

In Fig. 1 the temperature variability for the JJA (the standard deviation of the summer two meter temperature) period is reported for the three time slices and for both simulations coupled (left column) and uncoupled (right column).

It is evident for the coupled simulation the increase in temperature variability when the near (2021-2050) and far (2071-2100) future is compared with the present day period. The same comparison for the uncoupled simulation shows that the increase in temperature variability is much less or almost zero in some areas for both the near and far future.

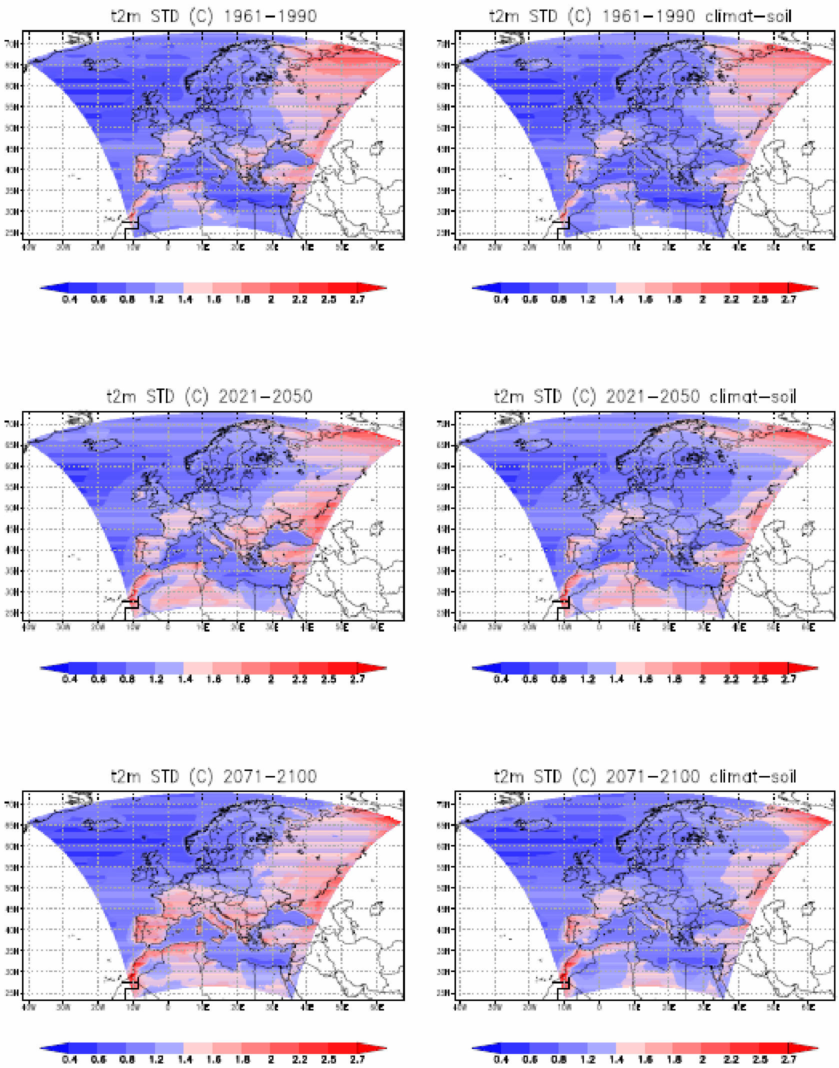

Figure 1.1: Standard deviation of summer (June–August) temperature in coupled (left column), uncoupled (right column), present day (top row), near future (middle row) and far future (bottom row).

This is more evident in Fig. 1.2 where the change of temperature interannual variability is shown for the near future compared to the present (top row) and the far future time slice (middle row) for the coupled (left column) and the uncoupled (right column) experiment. In particular the change of interannual variability in Eastern Europe for the near future is impossible to reproduce without the land-atmospehre coupling. The same it is true for the far future when the Mediterranean basin is considered. In this case the most part of the changes is due to the land-atmosphere feedback as is evident in the bottom panels of Fig. 1.2 where the differences for the far future coupled and uncoupled temperature variability is shown (left panel) an the differences between the far future temperature variability coupled and uncoupled change are reported.

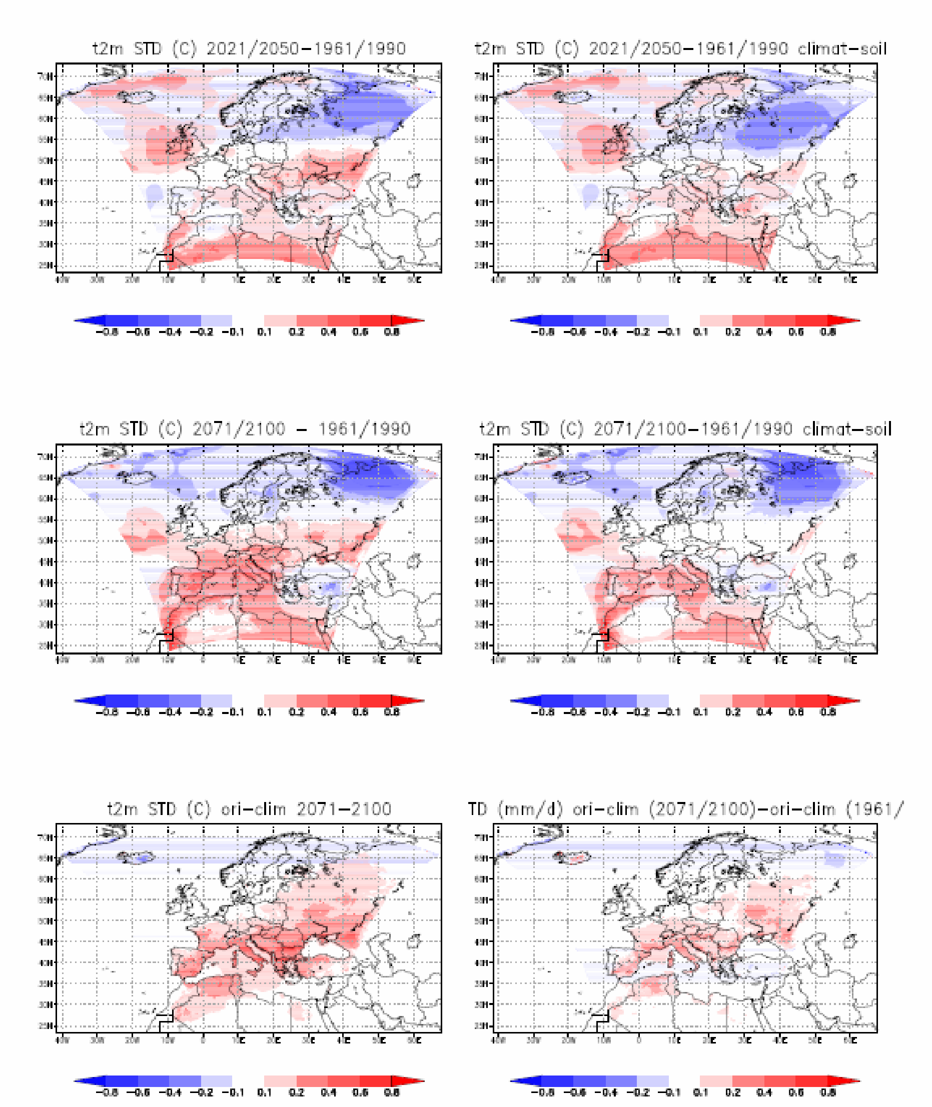

Figure 1.2: Changes in temperature standard deviation of the near and far coupled simulation (top and middle left column) and changes for the same period for the uncoupled simulation (top and middle right column). Difference for the far future coupled and uncoupled temperature variability (bottom left panel) and difference between the far future temperature variability coupled and uncoupled change (bottom right panel)

This results for temperature obtained so far confirm what has been previously found in Seneviratne et al. (2006) although the region for which the land-atmosphere coupling plays the main role is shifted more toward the south in the Mediterranean area compared to the previous results where the largest differences in the temperature variability change where observed in the central European region.

In Fig. 1.3 the same results as for Fig. 1.2 are reported but for the 10 km high-resolution simulations. In the top row the change in temperature variability for the far future are shown for the coupled and uncoupled simulation. For the Romania region the entire change in temperature variability is explained by the land-atmosphere coupling and the change in resolution doesn’t change the results already obtained in the 25 km simulation. This is more evident in the bottom row where again the differences for the far future coupled and uncoupled temperature variability are shown (left panel) and the differences between the far future temperature variability coupled and uncoupled change are reported. In this case the maximum differences are located in the South Romania and this is already evident in the 25km experiment. Therefore the high-resolution simulations show a kind of zoom of the signal already present in the original simulation.

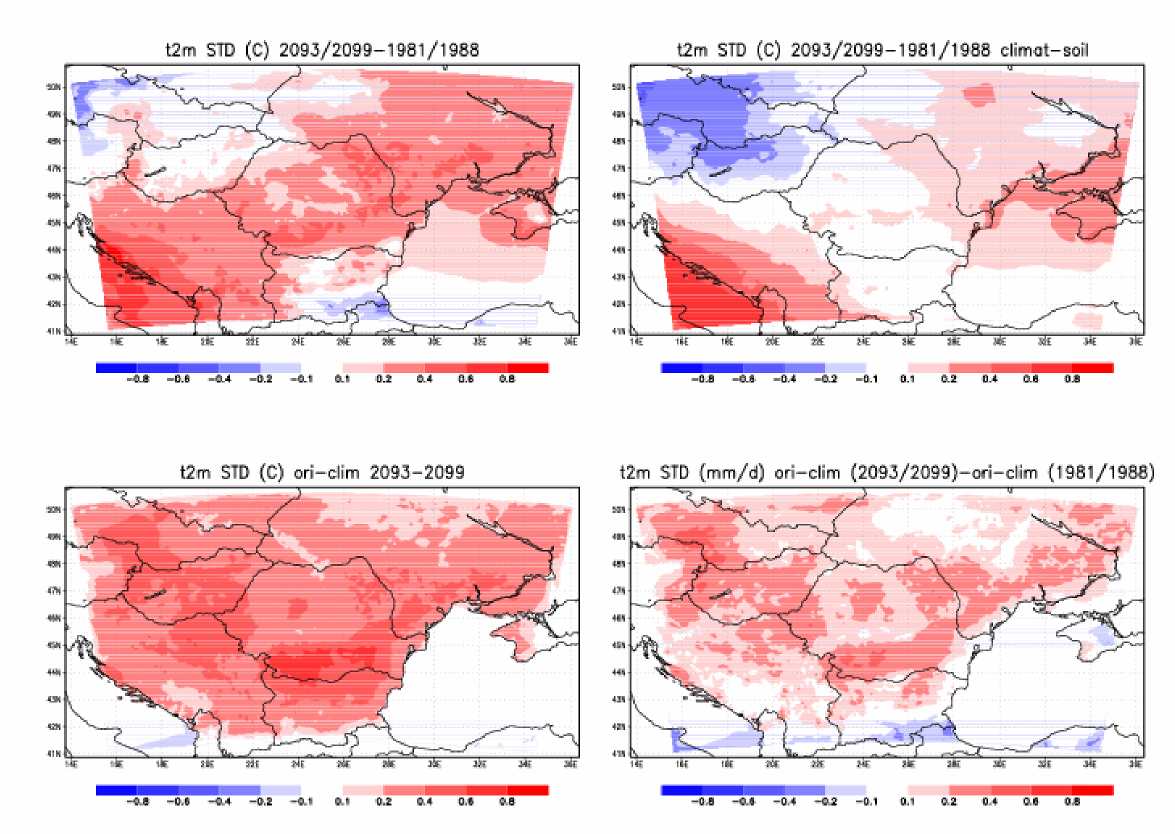

Figure 1.3: Changes in temperature standard deviation of the far future coupled simulation (top left column) and changes for the same period for the uncoupled simulation (top right column). Difference for the far future coupled and uncoupled temperature variability (bottom left panel) and difference between the far future temperature variability coupled and uncoupled change (bottom right panel)

1.3 Impact of land-atmosphere coupling on summer precipitation variability change

In Fig. 1.4 the same as Fig. 1.2 is reported but for the precipitation interannual variability computed as the coefficient of variation (standard deviation divided by the mean). For the precipitation the coupled and uncoupled experiments do not show any significant difference therefore we cannot conclude the same as for temperature regarding the role of land-atmosphere. This is confirmed also from the high resolution simulation reported in Fig. 1.5. These results are in partial contradiction with those found in Seneviratne et al. (2006), despite the similar signal found for temperature, but they confirm what has been found in the GLACE (Koster et al., 2006) experiment for the European region for precipitation (but not for temperature).

1.4 Conclusions

Both sensitivity experiments for the large European 25 km domain and the small 10 km domain of the Romania region highlight the importance of land-atmosphere coupling when temperature variability is concerned. In particular they indicate the Mediterranean basin as a hot spot where land-atmosphere feedbacks may play an importance role when future climate conditions are considered. The same analysis done for precipitation does not reveal any relevant effect of the land-atmosphere coupling at least in this experimental set-up.

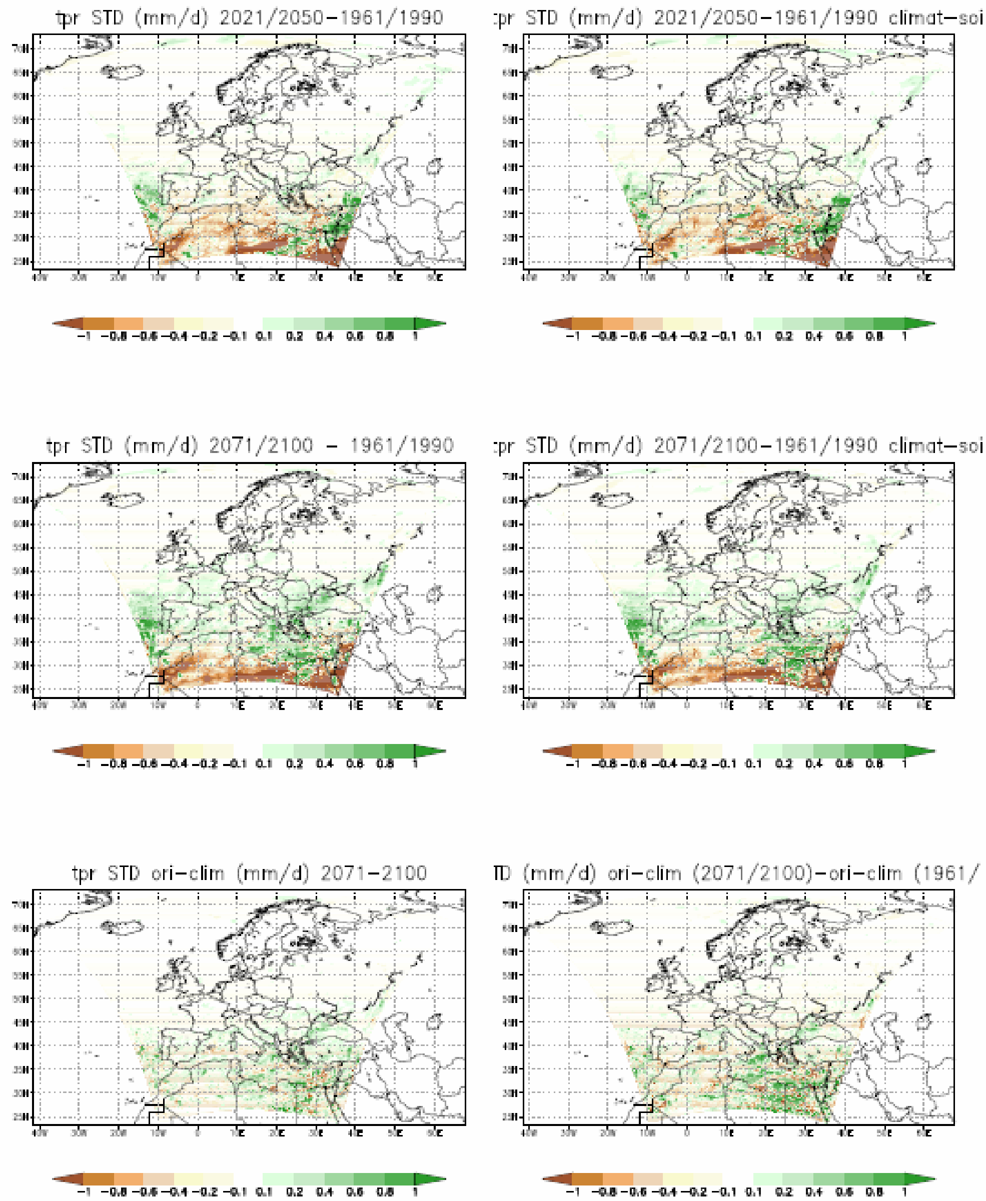

Figure 1.4: The same as Fig. 1.2 but for the precipitation coefficient of variation.

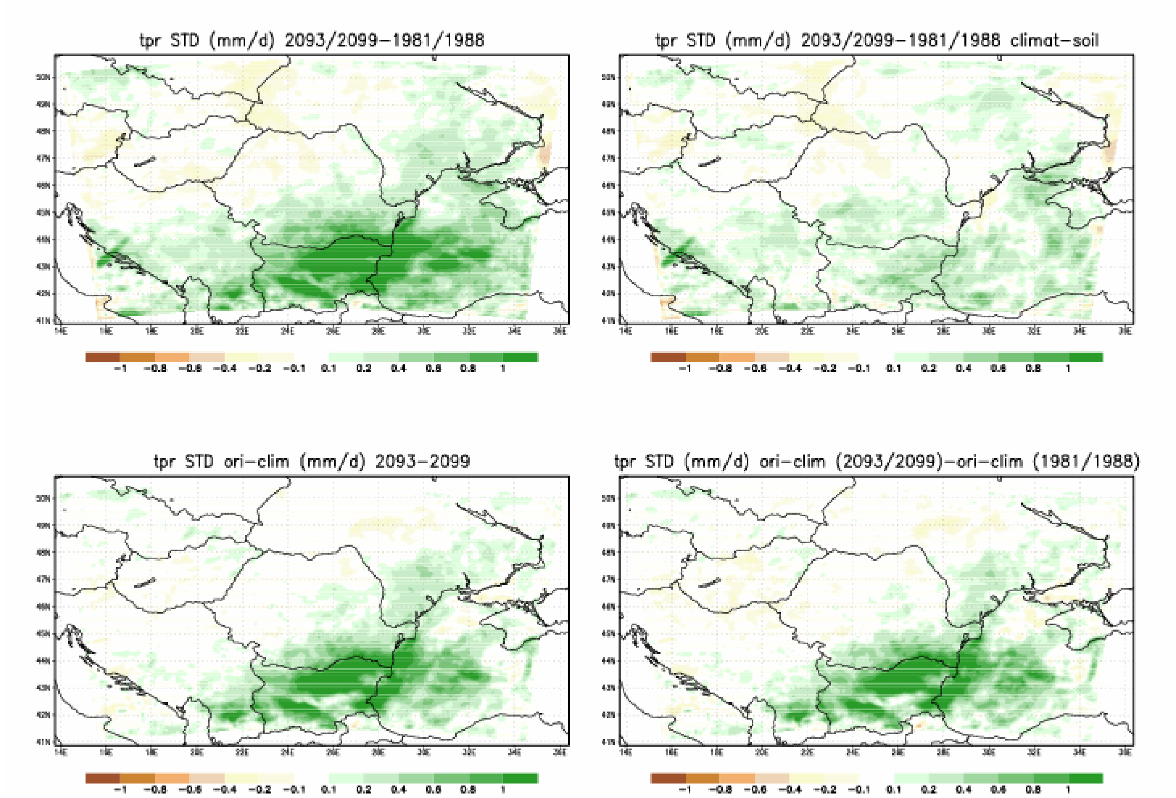

Figure 1.5: The same as Fig. 1.3 but for the precipitation coefficient of variation.

2. Impact of land surface processes for climate variability in Europe: Extremes and trends

For climate projections as well as for mid-range and seasonal weather forecasting, the importance of soil moisture as lower boundary condition for the atmosphere is being increasingly recognized. This is mostly due to the role of soil moisture as storage component for heat and moisture. The associated memory induces persistence in the overlying atmosphere. This has potential consequences for long-term forecasting, but only in regions where the atmosphere is coupled to the underlying land surface. This section provides an overview on a recent study (Jaeger and Seneviratne 2010) assessing the sensitivity of (summertime) extreme events to soil moisture in Europe using a regional climate model.

Soil moisture (SM) is a key variable of the climate system because of its impacts on the surface energy and water balances. This has consequences for the near-surface climate (temperature, humidity) as well as for boundary-layer processes (e.g. convective precipitation) and potentially also large-scale circulation patterns. Moreover, as a storage component for water and hence indirectly also for energy, it represents an important memory component for the regional climate system, with high potential for seasonal forecasting. It is however not routinely measured in most parts of the world, particularly in Europe, where measurement datasets are scarce (Seneviratne et al., 2010).

Since climate extremes have a major societal, economical, and ecological impact, they are of particular interest for society. Several observational (Della-Marta et al., 2007) and modeling studies (Meehl and Tebaldi, 2004) report an increase in temperature extremes in mid-latitude regions with climate change that can be linked (among other factors) to changes in soil moisture regimes (Seneviratne et al., 2006). However, soil moisture only impacts the surface climate in specific regions on earth, so called 'hot-spots' of land-atmosphere coupling (Koster et al., 2004). Since large-scale field experiments investigating land-atmosphere coupling effects are not feasible, one way of assessing the underlying mechanisms is to run climate model experiments.

Hereafter, we discuss results from a study conducted by ETH assessing the sensitivity of temperature and precipitation extremes and trends to the soil moisture state. This study uses output from regional climate model simulations run for the last 50 years over the European continent. The applied methodology is based on simulations with prescribed and interactive SM (similar as in e.g. Koster et al. 2004) and Seneviratne et al. 2006). This approach allows us to assess the impact of SM on climate by decoupling the land-surface part of the model from the atmospheric part, and thereby to infer causal relationships. In the simulations with prescribed SM the two-way coupling of the atmosphere and SM is removed, and the experiments thus investigate only the one-way effect of SM on the atmosphere, whereas the atmosphere has no influence on SM.

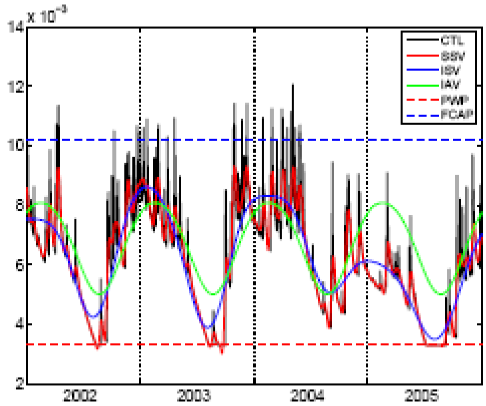

Figure 2.1: Illustration of the soil moisture evolution of the different CLM experiments for a randomly chosen grid point in the analysis domain. Shown is the 2nd model soil level for the period 2002-2005. [Jaeger and Seneviratne 2010]

2.1 Data and Methodology

The study uses the CLM RCM, which is the climate version of the non-hydrostatic COSMO model (Consortium for Small-scale MOdeling: http://cosmo-model.cscs.ch/). A similar model configuration is adopted as for the EU-FP6 project ENSEMBLES (http://www.ensembles-eu.org) validated in Jaeger et al. (2008).

In addition, the employed model setup was validated with regard to land-atmosphere coupling characteristics with FLUXNET observations in Jaeger et al. (2009). CLM is integrated over the European continent, with 0.44◦ (≈ 50 km) horizontal resolution, 32 levels in the vertical and 10 soil layers. Lateral boundary conditions are derived from the ERA40 re-analysis (1958-2001, Uppala et al. 2005) and from ECMWF operational analysis (2002-2006). The applied CLM configuration uses the Tiedtke convection scheme based on a moisture-convergence closure, which was shown to have a strong sensitivity of precipitation to evapotranspiration anomalies (see Jaeger and Seneviratne 2010 for a discussion). Details on the model dynamics and physics are provided in the model documentation (available from: http://www.clm-community.eu/).

In order to assess the possible impact of extreme values and of the temporal variability of SM on the European summer climate, a set of sensitivity experiments with different prescribed SM evolutions was performed (see Fig. 2.1 for an illustration of the SM values of the sensitivity experiments in comparison with the control simulation). Note that in the prescribed SM experiments, soil moisture is not altered by any surface fluxes, nor by precipitation or runoff. A reference simulation includes interactive SM, and will be referred to as CTL hereafter.

Two sensitivity experiments were performed with minimum (plant wilting point, PWP) and maximum (field capacity, FCAP) soil moisture values. In addition, the impact on climate of temporal SM variability on different time scales is assessed. In order to disentangle the effects of synoptic-scale, intraseasonal, and interannual SM variability, the soil moisture time series from CTL are subsequently filtered using a digital low-pass filter. A first experiment removes the synoptic-scale variability (called SSV) of SM. A second experiment additionally removes the intraseasonal variability (called ISV) from SSV. A third experiment also removes the interannual variability from ISV (called IAV).

2.2 Impact of soil moisture on the European summer climate

2.2.1 Impact on temperature extremes

While in Jaeger and Seneviratne (2010) several diagnostics for extreme events are assessed, we will focus hereafter only on heat wave duration indices (Fig. 2.2) as well as on the analysis of the PDFs of daily maximum temperatures (Tmax, Fig. 2.3). Figure 2.2 (top left panel) displays the mean heat wave duration index $hwdi_{mean}$ that assesses the atmospheric tendency for persistence at the upper tail of the daily Tmax distribution. It is calculated as the mean of all events with at least two consecutive days of Tmax above the long-term 90th-percentile of the CTL simulation. The 90th-percentile of each summer day is calculated from samples of 5 days (2 days before and 2 days after) over the full analysis period (1959-2006). Largest values occur in the Mediterranean and in Eastern and Northern Europe. Generally, the values of $hwdi_{mean}$ are higher for regions neighbouring oceans, possibly indicating an effect of persistence associated with SSTs. A comparison of the differences of $hwdi_{mean}$ between the sensitivity and CTL experiments yields the following: There is a continuous decrease from SSV over ISV to IAV, and most pronounced effects in FCAP and PWP (Fig. 2.2, top panels). It is likely that one cannot trust the strong impact of SM on the heat wave indices in Scandinavia, since Jaeger et al. (2009) found a poor representation of land-atmosphere coupling in Northern Europe in the applied CLM version. Finally, note that the biases of temperature extremes of CTL are comparable to those of current state-of-the-art RCMs from ENSEMBLES (see also Jaeger and Seneviratne 2010).

The index $hwdi^{\star}_{mean}$ (Fig. 2.2, bottom panels) is an indirect measure of intrinsic heat wave persistence. In contrast to $hwdi_{mean}$, it uses the long-term 90th-percentile of the respective simulation as threshold for the definition of heat wave days. If one compares $hwdi^{\star}_{mean}$ in two simulations, differences in this index can (mostly) only arise from the fact that the clustering of days above their respective 90th-percentile differs (in both simulations 10% of all days are above the 90th-percentile). As shown in Fig. 2.2, $hwdi^{\star}_{mean}$ exhibits clear reductions in the IAV, PWP and FCAP experiments. A more thorough analysis reveals that this is in line with a decrease in the autocorrelation of Tmax, and that the distribution of the length of 90th-percentile threshold exceedances shows an increase of shorter and a decrease of longer lasting heat wave episodes (for further details see Lorenz et al. 2010). This can be understood by the fact that in these simulations precipitation does not cause SM anomalies (prescribed SM). Hence, one source of atmospheric persistence, namely soil moisture memory, is shut down. We see from the response of the IAV experiment that it is the memory associated with interannual SM anomalies that is mostly relevant.

In Fig. 2.3 (left panel) we assess the PDFs of mean subdomain daily Tmax in Eastern Europe, using the subdomain definition of the EU-project PRUDENCE (e.g. Christensen and Christensen, 2007). Analyses for other European subdomains are provided in the supplementary information of Jaeger and Seneviratne (2010). Consistent with the previous analysis of the $hwdi_{mean}$ and $hwdi^{\star}_{mean}$ heat wave indices, largest differences of daily Tmax are found for PWP and FCAP. The analysis reveals that the Tmax PDFs of the PWP and FCAP simulations are significantly different from CTL (based on the two-sided Kolmogorov-Smirnov test, with a = 5%), which to a lesser extent also holds for ISV and IAV. At least for PWP, FCAP and IAV, not only the mean but also the tails or the spread of the distributions are significantly smaller. Interestingly, PWP (FCAP) exhibits a pronounced widening (narrowing) of its PDF, which is due to the removed (increased) damping effect of SM – through evaporative cooling – on the temperature extremes at the high end (i.e. hot extremes). The distinct impact of SM is clearly recognizable from the asymmetric effects on the PDFs.

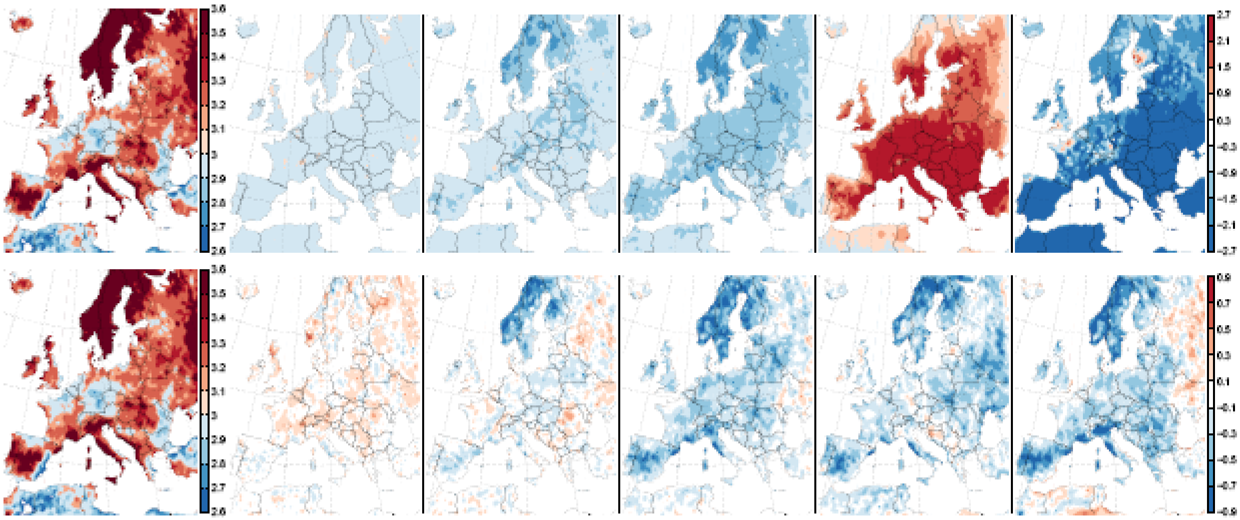

Figure 2.2: Summer climatologies (1959-2006) of the impact of SM variability on Tmax extreme diagnostics: $hwdi_{mean}$ (heat wave day threshold defined with respect to 90th-percentile of CTL, [d], 1st row) and $hwdi^{\star}_{mean}$ (heat wave day threshold defined with respect to 90th-percentile of respective experiment, [d], 2nd row). From left to right CTL, SSV-CTL, ISV-CTL, IAV-CTL, PWP-CTL and FCAP-CTL are shown. [Jaeger and Seneviratne 2010]

The right panel of Fig. 2.3 displays the corresponding PDFs of the extreme value distribution of daily Tmax (using the Generalized Extreme Value distribution (GEV) based on the block maxima approach (Coles, 2001, using summer (JJA) seasonal blocks). These PDFs are shifted to higher temperatures and they are narrower compared to the PDFs of daily Tmax discussed above. While the differences of the sensitivity experiments seem to be more pronounced, the statistical analysis reveals slightly lower significance (mainly due to the smaller sample size). As identified for the overall PDFs, we see that SM has a strong impact mainly on temperature maxima (the higher tails of the PDFs), which can be understood from the presence or lack of latent cooling.

In summary, we find that reducing the temporal soil moisture variability reduces the temperature extremes, and that it is the interannual variability of SM that is most relevant in this respect. Imposing extreme values of soil moisture has the largest impact. These effects are asymmetric and impact temperature maxima rather than the whole PDF, which is consistent with a non-linear dependency of surface fluxes on soil moisture (e.g. Koster et al., 2004, Seneviratne et al., 2010), i.e. the existence of distinct regimes with little vs. high sensitivity to soil moisture (in wet, respectively drier, soil moisture conditions).

2.2.2 Impact on precipitation extremes

In contrast to the results for daily Tmax, our results suggest that daily precipitation extremes are not significantly affected by temporal SM variability. Significant impacts are only found for the extreme experiments (PWP, FCAP) where the wet day frequency and consequently the absolute mean summer daily precipitation and also the 5-day maximum precipitation amount, all have larger values in the wet case due to increased frequency of days with convective precipitation. However, the wet day characteristics, as expressed by e.g. the wet day intensity (the average precipitation amount on rainy days, defined as > 1mm/day) or the 95th-percentile, are similar for all experiments (not shown).

Therefore, we only show the PDFs of mean (left panel) and extreme (right panel) subdomain daily precipitation in Eastern Europe in Fig. 2.4. Analyses for other European subdomains are again provided in the supplementary information of Jaeger and Seneviratne (2010). In contrast to the strong impact of SM on the PDFs of Tmax displayed in Fig. 2.3, the impact on precipitation is rather modest. Only the extreme experiments (PWP and FCAP) seem to be significantly impacted (but not for all subdomains considered), at least according to the two-sided Kolmogorov-Smirnov test (again α = 5%).

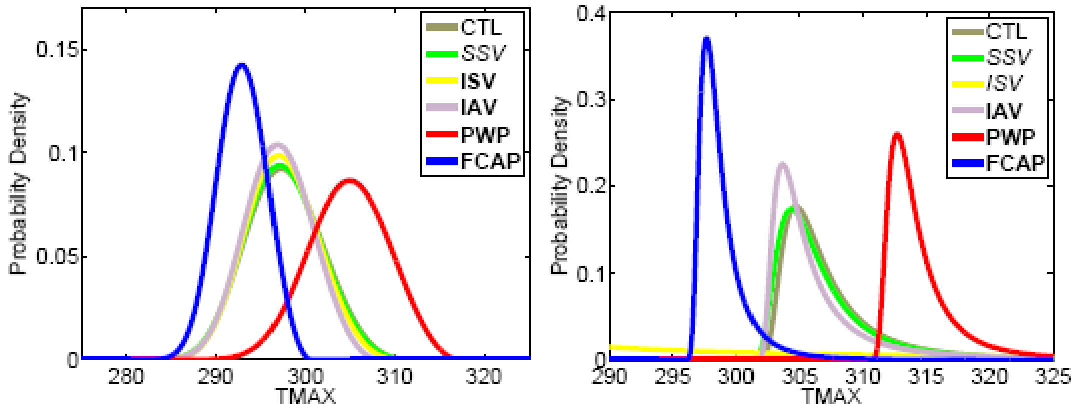

Figure 2.3: PDFs of daily Tmax [K] (left) and of summer Tmax block maximas [K] (right) using a GEV fit in both cases. The PDFs are based on the mean Eastern European subdomain values and the summer period 1959-2006. Simulations with bold legend entries are significantly different from CTL at the 5% level according to the two-sided Kolmogorov-Smirnov *test*. [Jaeger and Seneviratne 2010]

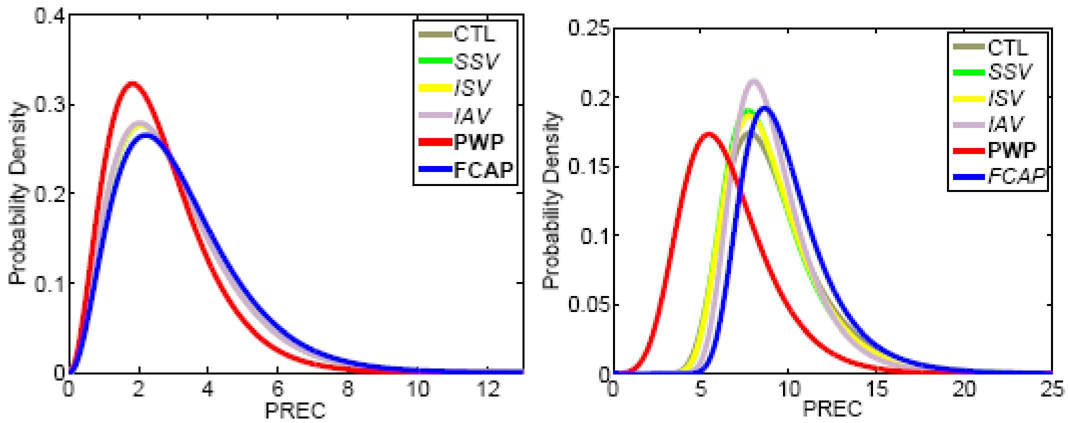

Figure 2.4: The same as in Fig.2.3 but for daily precipitation. [Jaeger and Seneviratne 2010]

2.2.3 Impact on trends

In this section we investigate trends in summer climate over the period 1959-2006 in the conducted experiments. Of particular interest is the question of whether changes in soil moisture characteristics may have any influence on these trends. Using the performed CLM experiments with and without prescribed SM, this can be easily assessed. We discuss here only the results for Tmax and cloud cover. Further results are provided in Jaeger and Seneviratne (2010). The analysis reveals that the trends are different for simulations with (CTL, SSV, ISV) and without (IAV, PWP, FCAP) SM trends, respectively. However, since there are no substantial differences (not shown) between trends for CTL, SSV and ISV, respectively IAV, PWP and FCAP, we only discuss here the trends for CTL and IAV.

We distinguish here two periods corresponding to the 'global-dimming/global-brightening' phases (e.g. Wild et al., 2005): 1959-1980 ('1*st* period') and 1981-2006 ('2*nd* period'). Figure 2.5 shows that there is a striking temporal variation in the Theil-Sen's trend estimates (trend estimator from the Mann-Kendall tau trend test) for the JJA seasonal mean of daily Tmax between the 1*st* and 2*nd* periods. For CTL there is a negative trend for the 1*st* period over the whole of Europe, and a positive trend for the 2*nd* period. For IAV there is a tendency for smaller negative and positive trends for the 1*st* and 2*nd* period, respectively (the numbers in the lower right corner denote the area-weighted fraction of land points with statistically significant trends according to the Mann-Kendall tau test, at the 10% level). The corresponding trends for Tmin exhibit similar spatial and temporal patterns but are weaker. Moreover, the differences between CTL and IAV are substantially smaller. Hence, SM (trends) unequally affect Tmax and Tmin (trends), with consequences for the DTR trends (not shown, see Jaeger and Seneviratne 2010).

Interestingly, these contrasting trends over the two analysed periods are found despite the fact that CLM does not explicitly include changes in aerosol concentrations. These are also not included in the driving boundary conditions (ERA40, ECMWF operational analysis). However, part of the local response could be due to changes in cloud cover induced by the imposed boundary conditions (i.e. changes in moisture or temperature fields - which could be indirectly due to aerosol trends – which are captured in the reanalysis/analysis datasets thanks to data assimilation, see also Hirschi and Seneviratne 2010).

Therefore, we also investigate the trends in CLM total cloud cover in Fig. 2.5. They exhibit the same spatial as well as temporal patterns (with an increase in the 1*st* period and a decrease thereafter) as the trends in daily Tmax. The SM trend patterns (both spatial and temporal) are similar to those of the cloud cover. Since cloud cover and SM interact with one another, it is difficult to assess their respective independent contributions to the temperature trends. However, by looking at those simulations without trends in SM (IAV, PWP, FCAP), one finds a small trend reduction (in particular for extreme values of Tmax, not shown). Therefore, we conclude that in CLM the trends of daily Tmax and of DTR (not shown) are mainly due to trends in cloud cover caused by the large-scale forcing (circulation patterns, as well as temperature and relative humidity of incoming air at the domain boundaries), and that SM has an amplifying effect. Finally, note that despite inconsistencies in the boundary data (e.g. the change from ERA40 re-analysis to ECMWF operational analysis in 2002, or the inclusion of satellite data assimilation in recent decades), a comparison with observed trends reveals a reasonable representation, at least qualitatively (see Jaeger and Seneviratne 2010).

2.3 Conclusions

This study briefly summarizes some of the highlights of a recently completed study (Jaeger and Seneviratne, 2010) that deals with the impact of different soil moisture settings on the European summer climate using the regional climate model CLM. Thereby, the focus is particularly set on the impact of SM on climate extremes and trends in both Eastern and Western Europe. The main results of this study are as follows: Temperature extremes, as investigated by climate extreme indices and PDFs, are strongly affected by the absolute value and to a smaller extent also by changes in temporal variability of SM. This is mainly due to intraseasonal as well as interannual SM variability, with largest impact over Scandinavia and Central Europe.

SM memory effects are found to be important for the intrinsic persistence of hot days (see also Lorenz et al. 2010). Moreover, the effect of SM on temperature is asymmetric with strongest impacts on temperature maxima.

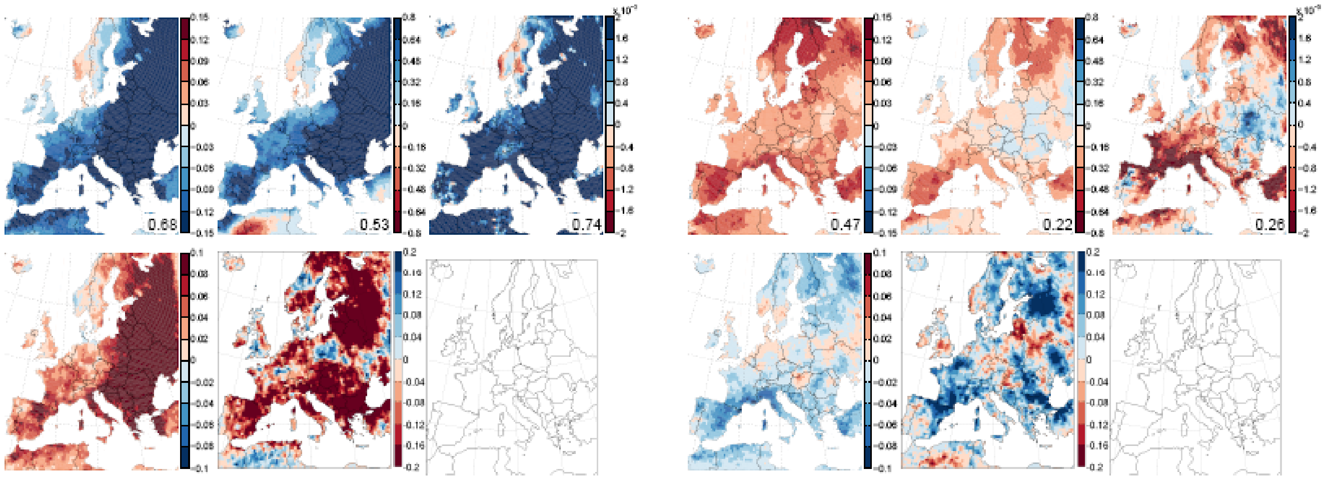

Figure 2.5: From left to right: Linear trends as expressed by Theil-Sen's trend estimate for mean daily Tmax [K/y], total cloud cover [%/y], and soil moisture [m/y] (for the 1. summer period 1959-1980); then the same but for the 2. summer period 1981-2006. From top to bottom: CTL and IAV-CTL. [Jaeger and Seneviratne 2010]

In contrast to the results for temperature, our results suggest that precipitation extremes are not significantly affected by temporal SM variability. Significant impacts are only found for the extreme experiments (PWP, FCAP) where the wet day frequency and consequently the absolute mean summer daily precipitation and the 5-day maximum precipitation amount, all have larger values in the wet case due to increased frequency of days with convective precipitation. However, the wet day characteristics, as expressed by e.g. the wet day intensity and the 95*th*-percentile, are similar for all experiments.

Trends of daily Tmax (as well as of extremes thereof) follow the 'global-dimming/global-brightening' trends in radiation in the experiments. In CLM, the trends are mostly due to trends in cloud cover, whereas SM acts as an amplifier. This is the case in the experiments, although they do not include directly observed trends in aerosols, but only possible indirect constraints through the boundary conditions. Trends in the extremes of Tmax are particularly affected by SM trends. The latter result suggests that the increasing trend in temperature extremes is partly associated with a drying trend in SM.

In conclusion, this analysis has shown that soil moisture-climate interactions can have a significant effect on temperature (partly also on precipitation) extremes and trends for the European summer climate. In order to properly evaluate the model dependency of our results, it would be necessary to repeat the analysis using different RCMs in a multi-model framework.

3. Precipitation parameterization tuning in RegCM model

In the scope of the CECILIA project, experiments were carried out at CUNI trying to find possible further reduction of precipitation bias. First experiment of the set was based on adjusting the internal parameters *rh0land* and *rh0oce* in RegCM „beta" version, the second one described in this report used a modified function of fractional cloud coverage (s-shaped function) in RegCM „alfa" version. The period simulated was 1961 and values were averaged over the inner part of the CUNI domain (i.e., without the buffer zone).

3.1 *rh0land* adjustment

As the RegCM model gives very high precipitation values, even in the „beta" version, we tried tuning parameter *rh0land*, increasing its value from 0.8 to 0.9 and increasing parameter *rh0oce* value from 0.9 to 0.95.

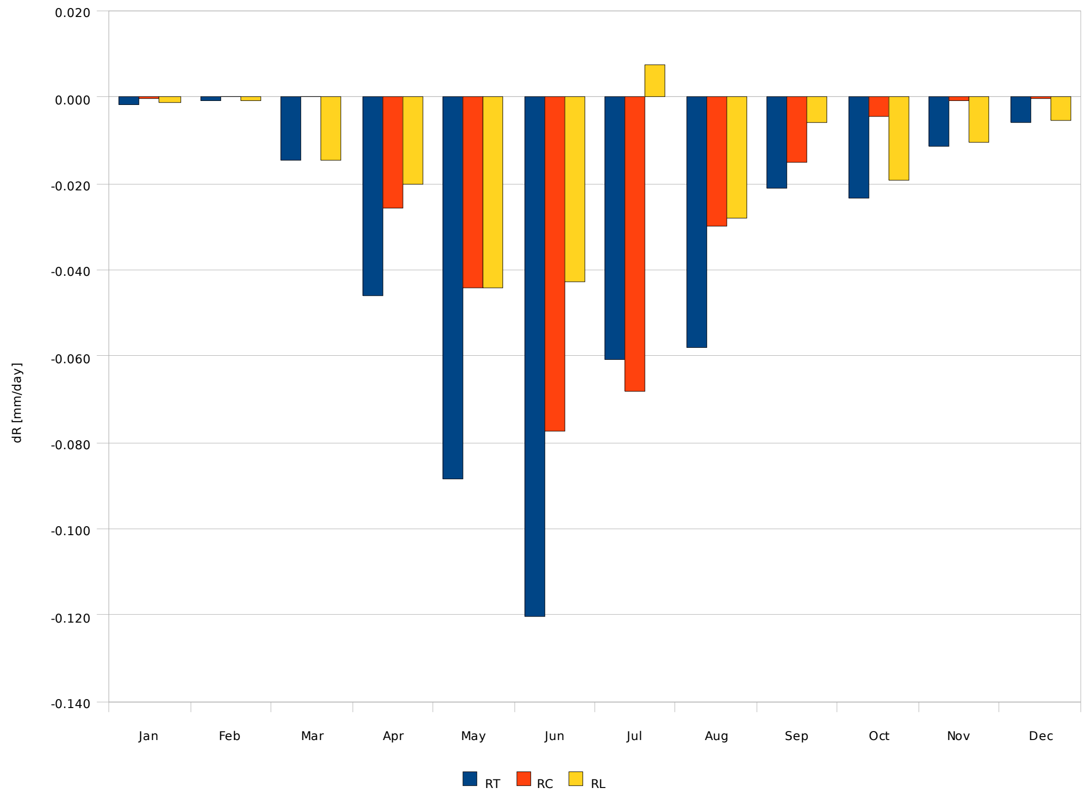

Figure 3.1: Precipitation change in adjusted model from original RegCM-beta, *rh0land* and *rh0oce* modified, RT = total precipitation, RC = convective precip., RL = large-scale precip.

The Fig. 3.1 shows, that the parameter adjustment results in precipitation reduction, but mainly in spring and summer part of the year, in July the reduction occurs only in convective precipitation, while large-scale precipitation increases. Even in the summer months, the precipitation change is small (less than 10 %).

3.2 s-shaped function of fractional cloud coverage

In this approach, a modified function of fractional cloud coverage is used as pictured in Fig. 3.2.

In this case, the precipitation values decrease only in May, June and July and this is caused again by the decrease in convective precipitation. The differences are around or even more than 10 %, but not in the desired direction in the rest of the year (Fig. 3.3).

3.3 Conclusions

Comparing the two experiments, we see that the simple modification of fractional cloud coverage parameters doesn't have the expected effect on precipitation. Both modifications end up affecting more the convection than large-scale precipitation. To get the intended bias reduction, more tuning needs to be done.

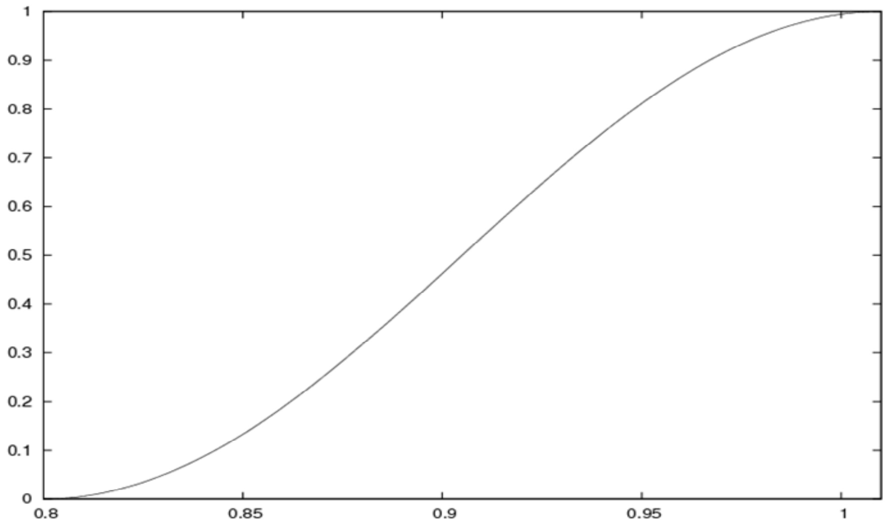

Figure 3.2: S-shaped function of fractional cloud coverage.

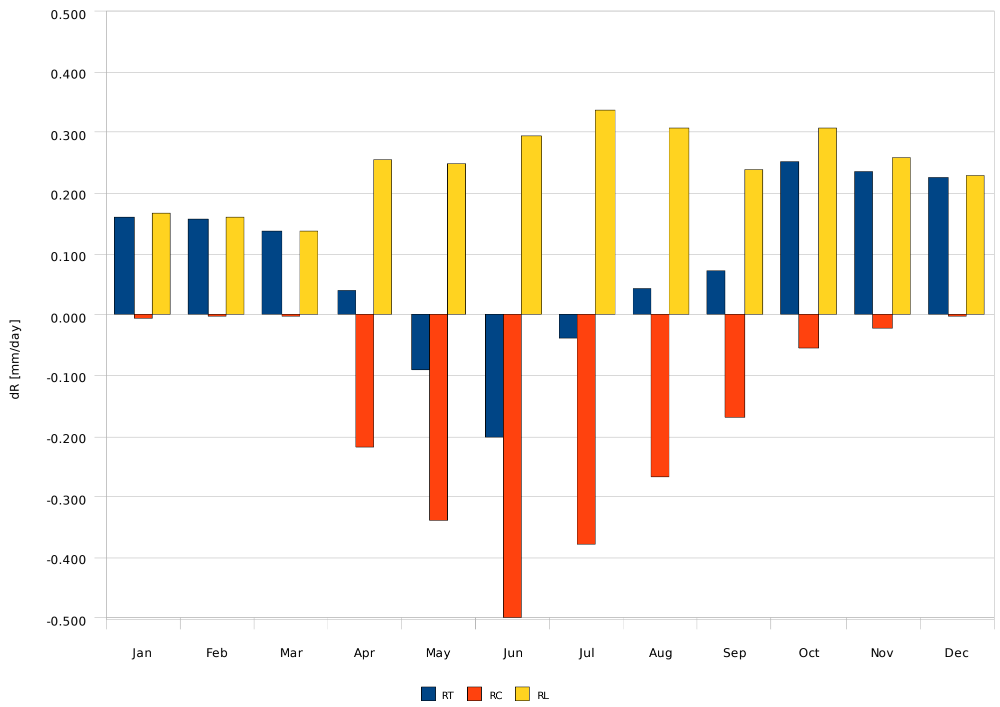

Figure 2.3: Precipitation difference between RegCM-alfa with original and modified fractional cloud coverage function.

References

Christensen, J. H, and O. B. Christensen (2007), A summary of the PRUDENCE model projections of changes in European climate during this century, *Clim. Change*, doi:10.1007/s10584-006-9210-7.

Coles, S. G. (2001), An introduction to statistical modeling of extreme values. Springer Series in Statistics, Springer, 224pp.

Della-Marta, P. M., M. R. Haylock, J. Luterbacher, and H. Wanner (2007), Doubled length of western European summer heat waves since 1880, *J. Geophys. Res., 112*, D15103, doi:10.1029/2007JD008510.

Hirschi, M., and S.I. Seneviratne, 2010: Intra-annual link of spring and autumn precipitation over France. *Climate Dynamics*, published online, doi: 10.1007/s00382-009-0734-1.

Jaeger, E. B., I. Anders, D. Lüthi, B. Rockel, C. Schär, and S. I. Seneviratne (2008), Analysis of ERA40-driven CLM simulations for Europe, *Meteorol. Z., 17*, 349-367.

Jaeger, E. B., R. Stöckli, and S. I. Seneviratne (2009), Analysis of planetary boundary layer fluxes and land-atmosphere coupling in the Regional Climate Model CLM, *J. Geophys. Res., 114*, D17106, doi:10.1029/2008JD011658.

Jaeger, E. B., and S. I. Seneviratne (2010), Impact of soil moisture-atmosphere coupling on European climate extremes and trends in a regional climate model, *Clim. Dynam.*, in press.

Koster, R. D. et al. (2004), Regions of strong coupling between soil moisture and precipitation, *Science, 305*, 1138-1140.

Koster, R. D. et al. (2006), GLACE: The Global Land–-Atmosphere Coupling Experiment. Part 1. Overview. J. Hydrometeor. 7, 590–610.

Lorenz R., E. B. Jaeger, and S. I. Seneviratne (2010), Persistence of heat waves and its link to soil moisture memory, *Geophys. Res. Lett.*, submitted.

Meehl, G. A., and C. Tebaldi (2004), More Intense, More Frequent, and Longer Lasting Heat Waves in the 21st Century, *Science, 305*, 994 - 997.

Seneviratne, S. I., D. Lüthi, M. Litschi, and C. Schär (2006), Land-atmosphere coupling and climate change in Europe, *Nature, 443*, 205-209.

Seneviratne, S. I., T. Corti, E. L. Davin, M. Hirschi, E. B. Jaeger, I. Lehner, B. Orlowsky, and A. J. Teuling (2010), Investigating soil moisture-climate interactions in a changing climate: A review, *Earth-Science Reviews*, in press.

Uppala, S. M., et al. (2005), The ERA-40 reanalysis, *Q. J. R. Meteorol. Soc., 131*, 2961-3012.

Wild, M., H. Gilgen, A. Roesch, A. Ohmura, C. Long, E. Dutton, B. Forgan, A. Kallis, V. Russak, and A. Tsvetkov (2005), From dimming to brightening: Decadal changes in solar radiation at the Earth's surface, *Science, 308*, 847-850.